

Revision 1

Discovery of zinc-rich mineral on the surface of lunar orange pyroclastic beads

Chi Ma¹, Yang Liu^{2,*}

¹Division of Geological and Planetary Sciences, California Institute of Technology, Pasadena, CA 91125, USA.

²Jet Propulsion Laboratory, California Institute of Technology, Pasadena, CA 91109, USA.

*Corresponding author: yang.liu@jpl.nasa.gov, 626-437-6532

Revised for: American Mineralogist as a Letter

Abstract: 249 words

Main text: 3908 words

Figures: 3

Table: 1

1 **ABSTRACT**

2 We present the first discovery of a Zn-rich mineral on the pristine surface of orange
3 pyroclastic beads from Apollo sample 74220. This Zn-rich mineral is wide occurring, trigonal or
4 hexagonal shaped, with a normalized composition of ~59 wt% Zn, ~26 wt% O (calculated), ~6
5 wt % S, ~5 wt % Na, and ~4 wt % Cl. The crystal morphology, homogeneity, and chemistry of
6 individual grains are most consistent with gordaite, a zinc chlorohydroxosulfate mineral, showing
7 an empirical formula of $\text{Na}_{1.02}\text{Zn}_{3.98}[(\text{SO}_4)_{0.84}(\text{OH})_{0.30}](\text{OH})_6[\text{Cl}_{0.50}(\text{OH})_{0.50}] \cdot n\text{H}_2\text{O}$, albeit the exact
8 amounts of OH and H₂O are uncertain. The pristine 74220 sample used in this study was only
9 exposed directly to air for a cumulative period of 16 days before our study. The same Zn-rich
10 crystals, examined 12 to 15 months apart, show no visible physical and chemical changes. Thus,
11 this zinc-rich mineral likely formed through rapid alteration (oxidation and hydration) by terrestrial
12 air of the original vapor-deposited Zn, Cl, S, and Na-bearing solids. The composition of zinc-rich
13 mineral indicates that the vapor condensates consist of metallic Zn and metallic Na with either
14 ZnS or native S, and either ZnCl₂ or NaCl. This is the first direct evidence that metallic Zn and
15 Na are key components in the vapor condensates of lunar volcanic gas, which implies lunar
16 volcanic gas may be under higher pressure than previously thought, and the gas composition may
17 be different than previously inferred. Our study is also relevant to collection, handling, curation,
18 and sample preparation of returned samples from other planetary bodies.

19 **Keywords:** Lunar orange beads, volcanic gas, vapor condensates, the Moon, zinc-rich mineral,
20 gordaite

21

INTRODUCTION

22 Lunar pyroclastic beads were produced in fire-fountain eruptions powered by gas exsolved
23 from partial melts of the deep lunar mantle (>250 km, e.g., Delano 1986; Meyer et al. 1975). These
24 primitive basaltic beads were reported to contain H and C residues after significant degassing (Saal
25 et al. 2008; 2013; Wetzel et al. 2015) and a surface coat rich in volatile elements condensed from
26 the gas (e.g., S, Zn, Cl), among which S and Zn are the most abundant (e.g., Meyer et al. 1975).
27 One of the key unanswered questions is how volatiles and volatile elements are lost from lunar
28 melts. The condensable species of Zn, S, and Cl depend on chemical compositions and physical
29 conditions of the volcanic gas, which major components are H, C, and S species (Renggli et al.
30 2017). As such, condensed S and Zn species on the surface of the beads would provide constraints
31 on chemical and physical conditions of the volcanic gas, and hence offer us the best opportunity
32 to study volatiles in the deep lunar interior. However, a host phase of condensable volatile
33 elements has never been revealed, despite of considerable surface analyses of pyroclastic beads in
34 1973-1993 (Butler 1978; McKay et al. 1973; Heiken and McKay 1974; Heiken et al. 1974; Chou
35 et al. 1975; Meyer et al. 1975; Butler and Meyer 1976; Goldberg et al. 1976; Wasson et al. 1976;
36 Tera and Wasserburg 1976; Clanton et al. 1978; Cirlin et al. 1978; Cirlin and Housley 1979;
37 Housley et al. 1979; McKay and Wentworth 1992). Here, we report the first observation of a host
38 mineral for Zn, S, Cl, and Na on the surface of orange beads from Apollo 17 soil 74220, using
39 advanced analytical field-emission scanning electron microscopy.

40

HISTORY OF THE SAMPLE

41 A small portion (~0.058 g) of pristine Apollo 17 soil 74220 was allocated for this work.
42 Unlike other lunar soils with light gray to dark gray color, soil 74220 is orange as it is nearly made
43 of pure orange glass (90 vol% of the soil is made of glass, Lunar Sample Compendium,

44 <https://curator.jsc.nasa.gov/lunar/lsc/74220.pdf>). A detailed process history of the allocated
45 sample was kindly provided by the Apollo Sample Curation Office at JSC (R. Zeigler, L. Watt,
46 Pers. Comm. on Sept. 11, 2018). Soil sample 74220 was collected in a Documented Bag (DB)
47 12E and placed into Sample Collection Bag (SCB) 8 carried by the astronauts on the lunar surface.
48 SCB 8 was put into a containment bag to protect the command module. The containment bag was
49 a beta cloth duffel bag with a draw-string mouth. The samples inside these bags were exposed to
50 air inside the lunar and command modules (pure O₂ with moisture from respiration) from five to
51 seven days with two to four depressurization-repressurization cycles on the Moon. On the
52 recovery ship in an isolated work area with filtered air, all of the SCBs were removed from the
53 containment bags, and all the returned containers (including DB 12E containing 74220) were
54 individually bagged in two Teflon bags and one polyethylene bag, all heat sealed (Dec. 1972).
55 During this step, samples were exposed to filtered air for nine to thirteen hours on the recovery
56 ship, and then were sealed in filtered air for about one and one-half days before being introduced
57 into nitrogen environment at the Lunar Receiving Laboratory (LRL), where these sealed bags were
58 unsealed in the nitrogen processing lines (cabinets). The parent sample (74220, 2) of our sample
59 was allocated to J.J. Katz on September 4, 1974 in a Pristine Sample Laboratory (PSL) Poly Vial
60 container, which was further sealed in two Teflon bags. This parent sample was returned unopened
61 on August 7, 1976. When returned, the sealed package (the original container and the sealed two
62 Teflon bags) was stored in the Returned Sample Storage in air until November 25, 2009 when it
63 was transferred into a PSL gas N₂ cabinet and split. The split sample was put in a plastic container,
64 which was again sealed in dry N₂ by two Teflon bags. This sealed package was then stored in the
65 Pristine Sample Vault (nitrogen) until it was shipped in May 2017. In summary, all pristine 74220

66 samples were directly exposed to 5-7 days in nearly pure O₂ and ~2 days in filtered air before
67 processing in the N₂ atmosphere in the LRL.

68 After we opened the double bags and sample container and prepared samples in 2017, the
69 first scanning electron microscope (SEM) session was performed within ~9 days. The remaining
70 sample stayed in the container in terrestrial air and used for additional SEM studies in 2017 and in
71 September 2018. Therefore, samples used in our first SEM session have been exposed directly to
72 pure O₂ and the terrestrial air for less than 18 days.

73 **METHODS**

74 We conducted analyses in three different sessions. In the first session in 2017, we opened
75 the double bags and container, picked 17 grains and placed them on a piece of carbon tape on one
76 SEM stub (~10 mm diameter, stub 1) around May 30th, 2017. The stub was carbon coated and
77 was examined on June 9th, 2017 using a Zeiss 1550 VP FE-SEM with an Oxford X-Max SDD
78 Electron Dispersive Spectrometer (EDS) system and a HKL electron back-scatter diffraction
79 (EBSD) system. A second SEM stub (stub 2) was prepared with 76 additional grains from the
80 open container, uncoated, and examined with the SEM in September 2017. Among the 93 grains
81 in the 2017 sessions, two are soil grains (aggregates), four are rock fragments, and the rest are
82 rounded beads (53) or broken glass shards (34). Only the outmost surfaces of 35 beads are visible,
83 whereas the remaining beads only display interior surfaces.

84 In the third SEM session in 2018, 19 beads were picked from the opened container, and
85 were pressed on a clean indium mount on September 12, 2018. In order to check carbon contents,
86 the indium mount was cleaned in the order of acetone, ethanol, and dichloromethane for 5-10
87 minutes, and then baked in vacuum (~6.7 x 10³ Pa) at 105 °C for ~7 days to remove organic
88 contamination. We performed SEM observations in 2018 on two beads in the indium mount and

89 two beads from the 2017 mounts (one from stub 1 and one from stub 2) to examine the changes of
90 the Zn-rich phase after they were exposed directly to terrestrial atmosphere for ~15 months. In
91 summary, in samples prepared for the SEM study, there are 54 beads with visible outer surfaces
92 and six soil grains.

93 In all SEM sessions, back-scatter electron imaging (BSE) was carried out in both high
94 vacuum and variable pressure (25 Pa) modes. EDS was used in high vacuum mode for quantitative
95 elemental analysis of the Zn-rich phase and other minerals on the lunar beads. These EDS data
96 were processed using the XPP correction procedure with Oxford factory internal standards. EBSD
97 analyses were performed on several large crystals of the Zn-rich mineral in 2017 and in 2018.
98 Owing to the rough curved surface of the beads, we did not attempt electron probe analysis of the
99 Zn-rich phase. Raman analysis was attempted with a Renishaw inVia™ Qontor Raman
100 Spectrometer with a green laser (512 nm) at 1 mW power.

101 RESULTS

102 We observed a Zn-rich mineral in the first SEM session of 2017. Further examination
103 showed that Zn-rich mineral occurs on the outer surface of 15 beads out of 37 beads studied, but
104 did not occur on the fractured interior surfaces nor on the surface of non-bead, soil or rock grains
105 (Figs. 1 and 2). Nanometer-sized dendritic pyroxene, metallic Fe (Fe⁰), and skeletal chromium-
106 bearing ulvöspinel are visible on and near the surface of beads, and often lie underneath the Zn-
107 rich phase (Figs. 1 and 2). The same zinc chlorohydroxosulfate grains did not display visible
108 changes after exposed to the ambient air for 15 months (Figs. 2 and S3).

109 The Zn-rich crystals appear to be a single phase (uniform brightness in BSE images) with
110 a trigonal or hexagonal shape, and are typically <3 μm in the largest dimension and <1 μm in
111 thickness (Figs. 1, 2, S1, and S2). These Zn-rich crystals are highly electron beam sensitive. As

112 a result, we were not able to obtain any EBSD pattern. Raman analysis of several Zn-rich minerals
113 also did not yield any Raman feature, although Raman analysis of glass suggests presence of
114 olivine and pyroxene. The EDS analysis of the Zn-rich mineral on all examined beads showed
115 that it contains Zn, O, S, Cl, and Na with variable amounts of contamination from the underlying
116 glass. The ~1 μm thick aggregates in Figure S2 display the least contamination from the glass
117 (Fig. 3). The normalized composition from a representative EDS analysis of this aggregates is:
118 ~59 wt% Zn, ~26 wt% O (calculated), ~6 wt % S, ~5 wt % Na, ~4 wt % Cl , and 0.4 wt% Mg
119 (Table 1). The Mg is possibly derived from the underneath glass. Glass without the
120 trigonal/hexagonal Zn-rich mineral contains ~0.1 wt% S and 0.5-1 wt% Na with no detectable Zn
121 and Cl (e.g., Fig. 3). The atomic ratios of Zn/Na (~4) and Zn/S/Cl (~8/~1.7/1) of the Zn-rich
122 aggregates remain unchanged at different excitation voltages of 15, 10, and 6 kV. These results
123 confirm that the Zn-rich mineral is a single phase. Further, EDS analysis of beads mounted in
124 indium shows no detectable carbon (Fig. 3). Therefore, the most likely mineral is gordaite,
125 $\text{NaZn}_4(\text{SO}_4)(\text{OH})_6\text{Cl}\cdot 6\text{H}_2\text{O}$, which is the only known zinc salt containing all the observed elements
126 and is also hexagonal. By charge balance of the observed elements with oxygen and OH, we
127 calculated an empirical formula of the Zn-rich mineral as
128 $\text{Na}_{1.02}\text{Zn}_{3.98}[(\text{SO}_4)_{0.84}(\text{OH})_{0.30}](\text{OH})_6[\text{Cl}_{0.50}(\text{OH})_{0.50}]\cdot n\text{H}_2\text{O}$, which contains significant deficiencies
129 at SO_4^{2-} and Cl^- sites than the ideal gordaite. Without direct identification of its crystal structure,
130 we will refer to this Zn-rich mineral as zinc chlorohydroxosulfate in the following text. Among
131 all the beads studied, we did not observe ZnS, NaCl, FeCl_2 , or native S (S^0).

132

DISCUSSION

133 This is the first report of Zn, Cl, Na, S, and O occurring as one mineral phase, a zinc
134 chlorohydroxosulfate (likely gordaite), on lunar orange beads. Sulfate was indicated in two early

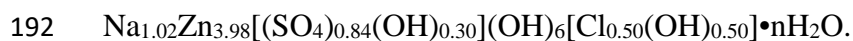
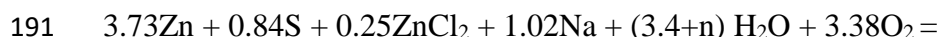
135 studies (Cirlin et al. 1978; McKay and Wentworth 1992). A third study by Clanton et al. (1978)
136 reported Na-Zn-Cl or Na-Zn-S in surface coating and euhedral NaCl grains on 74001/2 beads.
137 However, the SEM-EDS instrument used in Clanton et al. (1978) was incapable to detect oxygen.
138 McKay and Wentworth (1992) observed Zn (\pm Na)-S-O association on 74220 and 74001/2 beads.
139 Although Zn and Na were suspected to occur together, the instrumentation used in the 1992 study
140 cannot distinguish Zn *L* and Na *K* peaks. The X-ray photoemission spectroscopy of 74001 orange
141 beads by Cirlin et al. (1978) showed that a portion of sulfur was in oxidized form, but it is unclear
142 what is associated with SO₄²⁻. The observation of zinc chlorohydroxosulfate on the surface of
143 74220 beads in this study is rather unexpected, considering our sample likely experienced the
144 shortest exposure to terrestrial air than those in previous two studies. The samples studied by
145 McKay and Wentworth (1992) had been exposed to the ambient air since 1978. Although these
146 authors reported secular changes on the samples, a phase containing Zn, Na, S, and Cl was not
147 observed. The study by Cirlin et al. (1978) published ~6 years after Apollo 17 samples returned
148 to Earth, although it is unclear if the samples were sealed in N₂ before their measurements. Our
149 sample and those in early studies experienced the same exposure history before they arrived at the
150 Lunar Receiving Lab at JSC, but our sample was directly exposed to the terrestrial air for <9 days
151 before observing the zinc chlorohydroxosulfate in the first SEM session. We exclude the
152 possibility that the zinc chlorohydroxosulfate is terrestrial contamination. Natural occurrences of
153 gordaite on Earth have only been confirmed in sulfide chimneys from Juan de Fuca ridge and the
154 Edmond hydrothermal field, Central Indian Ridge, via reactions between discharging
155 hydrothermal fluids and sea water (Brett et al. 1987; Nasada et al. 1998; Wu et al. 2016), or in a
156 hydrothermal vein in San Francisco Mine, Chile (Schlüter et al. 1997). Gordaite is a common

157 product of Zn corrosion in Marine environments (e.g., Odnevall and Leygraf 1993). However,
158 based on the lunar sample record, our sample never came in contact with Zn metal.

159 Zinc chlorohydroxosulfate in our study, however, is likely an alteration product of vapor-
160 deposited Zn, Cl, S, and Na-bearing solids clustered on the surface of volcanic beads. Although
161 the mantle source of 74220 beads is more water rich among Apollo basalts (Hauri et al. 2011;
162 Chen et al. 2015), the amount of water in zinc chlorohydroxosulfate is unlikely sourced from the
163 volcanic gas in lunar fire-fountain eruptions, especially when H₂ is the dominant H species in the
164 volcanic gas (e.g., Renggli et al. 2017). Because the zinc chlorohydroxosulfate in our sample did
165 not show visible changes after being exposed in the terrestrial air for ~15 months, we further
166 suggest zinc chlorohydroxosulfate formed within the 18 days exposure to ambient air. The
167 formation of zinc chlorohydroxosulfate probably started when the samples were exposed to the
168 atmosphere in command and surface modules (pure O₂ with some moisture), or to the filtered
169 marine air before they were sealed in dry N₂. The rapid reaction with terrestrial air is supported
170 by a terrestrial-like hydrogen isotope signature of 74220 samples measured in 1973 (Epstein and
171 Taylor 1973). Moreover, after sealing in dry N₂, the reaction could have continued with trace
172 moisture diffused into the container while the sealed-double bag was sitting in the air. Terrestrial
173 experiments show that formation of zinc chlorohydroxosulfate is rapid, within days of exposure of
174 metal Zn to marine environments with Na, Cl, and SO₄ derived from sea water (Oodnevall and
175 Leygraf 1993; Coles et al. 2008; Diler et al. 2014). Since sample 74220 had never been in direct
176 contact with sea water or its spray, Na, Cl, and S in the zinc-rich mineral are not terrestrial.
177 Moreover, the alteration of vapor condensates appears to be complete, because of the lack of Zn
178 and Cl in areas without the Zn-rich mineral and the absence of additional Zn, Na, Cl, and S species

179 on multiple beads. Therefore, from the composition of the zinc-rich mineral, we derive that vapor
180 condensates on 74220 beads are composed of Zn, Na, S, and Cl in an atomic ratio of ~8:~2:~1.7:1.

181 The solid species of these elements in the vapor condensates can be assessed using the
182 composition of the vapor condensates. Because the atomic abundances of Zn and Na are in excess
183 with respect to S and Cl, the vapor condensates would contain metallic Zn (Zn^0) and metallic Na
184 (Na^0), as previously hypothesized by Cirlin et al. (1978). The solid phases of S and Cl may be
185 present as S^0 or ZnS, and $ZnCl_2$ or NaCl, respectively. Differentiating between S^0 versus ZnS and
186 $ZnCl_2$ versus NaCl will require samples that have not seen any type of terrestrial air. Considering
187 the hydration and oxidation required to form zinc chlorohydroxosulfate, S^0 and $ZnCl_2$ are the most
188 likely candidates. Among all possible reactions of different species, the extreme hygroscopic
189 nature of $ZnCl_2$, the reactivity of S^0 and Na^0 , and the lowest Gibbs free energy make the following
190 reaction most likely:



193 Although S is one of the major volatile components of lunar volcanic gas, most of S is likely lost
194 as $S_{2(g)}$ or $H_2S_{(g)}$, and only a small amount was deposited as native S^0 or ZnS on the surface of lunar
195 beads (Renggli et al. 2017).

196 IMPLICATIONS

197 Our results have several implications, from volcanic degassing on the Moon to processing
198 of returned planetary samples on Earth. First, our results provide new insights in lunar volcanic
199 degassing inferred from Zn and Cl isotope signatures (Moynier et al. 2006; Herzog et al. 2009;
200 Sharp et al. 2010; Paniello et al. 2012; Kato et al. 2015). The Zn and Cl isotope compositions of
201 lunar basalts and pyroclastic beads indicate that the Moon experienced significant loss of volatiles

202 and volatile elements, and Zn and Cl were likely lost in the form of ZnCl₂, FeCl₂, and NaCl
203 (Moynier et al. 2006; Herzog et al. 2009; Sharp et al. 2010; Paniello et al. 2012; Kato et al. 2015).
204 However, the absence of FeCl₂ or NaCl on samples studied, the deficiency of Cl relative to Na and
205 Zn, and our inferred composition of vapor condensate imply that ZnCl₂ (and other metal chlorides)
206 is a minor vapor and solid phase compared to metallic forms of Zn and Na in the volcanic gas
207 associated with lunar fire-fountain eruptions, which further suggests the Zn and Cl degassing is
208 likely decoupled. Detailed examination of Zn and Cl isotope data of 74220 samples reveal some
209 interesting issues. Depletion of heavy Zn isotopes of bulk 74220 sample ($\delta^{66}\text{Zn} = -3.37$ and -
210 3.83 ‰) was explained by the presence of ZnCl₂ condensates in the sample (Paniello et al. 2012),
211 whereas enriched chlorine isotopes of bulk 74220 sample ($\delta^{37}\text{Cl} = +8.6$ and $+9.3$ ‰) are proposed
212 to be caused by significant degassing of ZnCl₂, FeCl₂, and NaCl (Sharp et al. 2010). If bulk 74220
213 sample contains condensed ZnCl₂, we would expect that Zn and Cl isotopes show similar
214 enrichment or depletion of heavy isotopes. The opposite trend of the Zn and Cl isotope
215 compositions of bulk 74220 sample implies either the effects of other non-volcanic processes such
216 as impact volatilization or sample preparation (see below), or Zn and Cl degassing is decoupled.
217 However, whether Zn and Cl degassing is decoupled for 74220 cannot be fully ascertained from
218 the available data, because isotope measurements on pure beads from sample 74220 are needed.
219 Moreover, all Zn measurements of sample 74220 did not analyze leachates (Moynier et al. 2006;
220 Herzog et al. 2009; Paniello et al. 2012), whereas some of the surface Zn, if not all, are likely
221 dissolved. In fact, this possibility is supported by the work of Day et al. (2017), the leachates using
222 water of two lunar rocks contain much higher Zn than the residues (Table S2 in Day et al. 2017).

223 Second, recent discoveries of residual H in pyroclastic beads and melt inclusions suggest
224 that mantle sources for these primitive magmas are likely water rich (Saal et al. 2008; 2013; Hauri

225 et al. 2011; Chen et al. 2015). This inference appears to contradict dry conditions required for
226 degassing of metal chlorides (Sharp et al. 2010). Decouple of Zn and Cl degassing from other
227 volatile elements, high Zn and Cl abundances in pyroclastic beads with directly measured high H
228 contents in melt inclusions (Hauri et al. 2011), and the loss of H as $H_2(g)$ other than $H_2O(g)$ (e.g.,
229 Renggli et al. 2017) would indicate that a water-rich mantle source for pyroclastic beads does not
230 prohibit degassing of Zn and Cl.

231 Third, our results can be used to evaluate the thermochemical model of volcanic gas by
232 Renggli et al. (2017). The model by Renggli et al. (2017) assumed that the melt contains volatiles
233 similar to those reported in Saal et al. (2008) and Wetzel et al. (2015). Based on thermodynamics,
234 Renggli et al. (2017) calculated the stable gas and solid condensate species at different conditions
235 (IW-2, IW, 10^{-6} bar, 1 bar). Their results show that zinc exists in the gas in the native form ($Zn_{(g)}$),
236 but condenses dominantly as ZnS via reaction with $S_{2(g)}$ under all calculated conditions (IW-2, IW,
237 10^{-6} bar, 1 bar). At the higher gas pressure (1 bar), metallic Zn appears as a minor solid species.
238 Contrast to the model predictions, our results imply that zinc condenses dominantly as Zn^0 . The
239 difference between model predication and our observation implies revisions of the assumptions in
240 the model: lunar melt contains significantly less sulfur and hence less $S_{2(g)}$ in the volcanic gas, or
241 most sulfur was lost before Zn condensed, or lunar volcanic gas had higher pressures. Presence
242 of a hot gaseous cloud during the fire-fountain eruption was also indicated based on the heat
243 capacity and cooling rate of 74220 beads (Hui et al. 2018). Therefore, metal Zn as the main species
244 of zinc condensed from the vapor is consistent with a gas cloud that facilitates separation of S_2
245 (and Cl species) from Zn.

246 Fourth, our results also suggest that sample preparation techniques used in bulk sample
247 analysis, especially for volatile elements, need to pay special attention to the soluble condensates.

248 Considering the rapid reaction with ambient air, exposure durations of pristine samples to ambient
249 air before analyses need to be documented and reported. Moreover, leachates of samples will need
250 to be analyzed for volatile elements (e.g., Zn, Pb, Cu). As shown above, sample preparation in Zn
251 analysis involved cleaning of samples in HCl (Moynier et al. 2006; Herzog et al. 2009) or double-
252 distilled water (Paniello et al. 2012), but the leachates were not analyzed in these studies. As a
253 result, the reported 140-254 ppm values in these studies likely underestimate the concentrations of
254 the vapor condensed Zn in bulk 74220 sample. Using the chlorine concentration in the leachate
255 of bulk 74220 sample (50 ppm, Sharp et al. 2010), and the inferred atomic Zn/Cl ratio of 8 from
256 our study, we inferred the surface Zn in bulk 74220 to be ~737 ppm. Furthermore, for vapor
257 condensates from the volcanic gas, measurements of pure glass beads from 74220 for both Zn and
258 Cl concentrations and isotopic values are needed.

259 Results from this study are also highly relevant to collection, handling, and curation of
260 returned samples from other planetary bodies. Surface mineralogy, chemistry, and reactivity of
261 returned samples are not only interesting to science (volcanic or impact processes) but also
262 important for future human explorations. The rapid alteration of vapor condensates as reported in
263 this study indicates that samples need to be kept in the state they are collected in (e.g., in vacuum
264 for the Moon and asteroids, or similar atmosphere they are collected on Mars). Investigations of
265 surface mineralogy, chemistry, and reactivity need to be performed as soon as sample containers
266 are open to the terrestrial air. Moreover, samples stored for future analysis need to be kept in an
267 environment similar to their host bodies. To fully resolve the solid species in the vapor
268 condensates, we will need to study pristine samples sealed under vacuum since their collection on
269 the Moon. NASA's plan to open these samples offers an excellent opportunity to resolve
270 uncertainties caused by terrestrial alteration. Maintaining the pristine states of these vacuum-

271 sealed samples during sample handling and processing is critical to the study of vapor condensates
272 on volcanic beads in these samples. The development of sampling handling approaches will be
273 highly beneficial to samples that will be returned from asteroids and Mars.

274 **ACKNOWLEDGEMENTS**

275 A portion of the work was performed at Jet Propulsion Laboratory, which is managed by
276 California Institute of Technology (Caltech) under a contract with NASA. We thank Ryan
277 Zeigler, Linda Watts, and Andrea Mosie from JSC Lunar Curation Office for tracking down the
278 process history of samples allocated for this work, George Rossman for running Raman analysis
279 on the Zn-rich mineral, and Liong Ma for helping with SEM and EDS analyses. YL
280 acknowledges the partial support by NASA Cosmochemistry grant NNN13D465T. SEM, EDS
281 and EBSD analyses were carried out at the Caltech GPS Division Analytical Facility, which is
282 supported, in part, by NSF Grants EAR-0318518 and DMR-0080065. We are grateful to the
283 constructive comments by an anonymous reviewer, David Pyle, and Ts. Stanimirova.
284

285

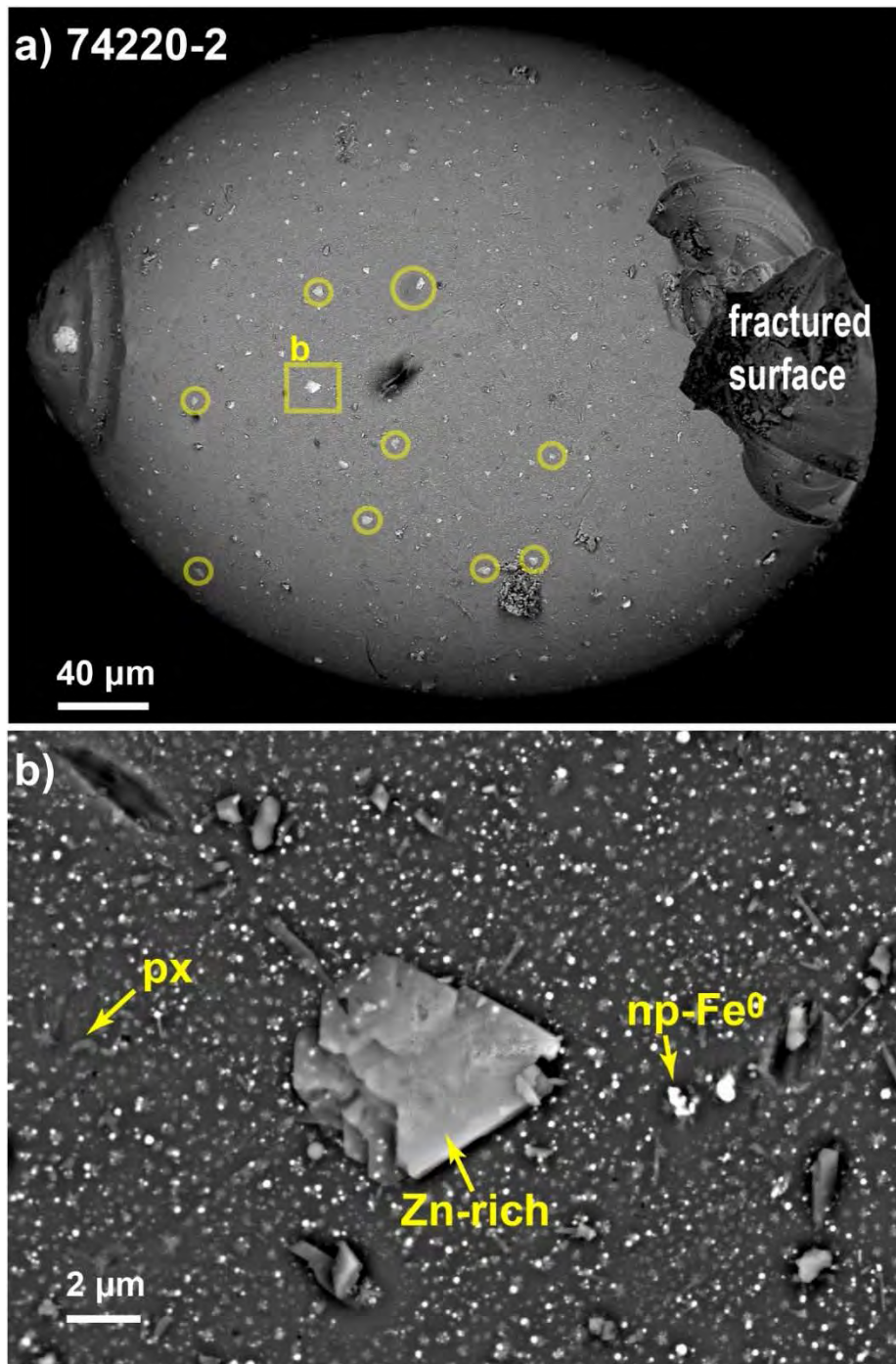
REFERENCES CITED

286

- 287 Brett, R., Evans, H.T., Gibson, E.K., Hedenquist, J.W., Wandless, M.V., and Sommer, M.A.
288 (1987) Mineralogical studies of sulfide samples and volatile concentrations of basalt
289 glasses from the southern Juan de Fuca Ridge. *Journal of Geophysical Research: Solid*
290 *Earth*, 92(B11), 11373-11379.
- 291 Butler, P., Jr. (1978) Recognition of lunar glass droplets produced directly from endogenous
292 liquids: The evidence from S-Zn coatings. In: *Lunar and Planetary Science Conference*,
293 9th, Houston, Tex., March 13-17, 1978, Proceedings. Volume 2. (A79-39176 16-91) New
294 York, Pergamon Press, Inc., 1978, p. 1459-1471.
- 295 Butler, J., Jr., and Meyer, C., Jr. (1976) Sulfur prevails in coatings on glass droplets: Apollo 15
296 green and brown glasses and Apollo 17 orange and black (devitrified) glasses. In: *Lunar*
297 *Science Conference*, 7th, Houston, Tex., March 15-19, 1976, Proceedings. Volume 2.
298 (A77-34651 15-91) New York, Pergamon Press, Inc., 1976, p. 1561-1581.
- 299 Chen, Y., Zhang, Y., Liu, Y., Guan, Y., Eiler, J., and Stolper, E.M. (2015) Water, fluorine, and
300 sulfur concentrations in the lunar mantle. *Earth and Planetary Science Letters*, 427, 37-
301 46.
- 302 Chou, C.L., Boynton, W.V., Sundberg, L.L., and Wasson, J.T. (1975) Volatiles on the surface of
303 Apollo 15 green glass and trace-element distributions among Apollo 15 soils. In: *Lunar*
304 *Science Conference*, 6th, Houston, Tex., March 17-21, 1975, Proceedings. Volume 2.
305 (A78-46668 21-91) New York, Pergamon Press, Inc., 1975, p. 1701-1727.
- 306 Cirlin, E.H., and Housley, R.M. (1979) Scanning Auger microprobe and atomic absorption
307 studies of lunar volcanic volatiles. In: *Lunar and Planetary Science Conference*, 10th,
308 Houston, Tex., March 19-23, 1979, Proceedings. Volume 1. (A80-23557 08-91) New
309 York, Pergamon Press, Inc., 1979, p. 341-354.
- 310 Cirlin, E.H., Housley, R.M., and Grant, R.W. (1978) Studies of volatiles in Apollo 17 samples
311 and their implication to vapor transport processes. In: *Lunar and Planetary Science*
312 *Conference*, 9th, Houston, Tex., March 13-17, 1978, Proceedings. Volume 2. (A79-
313 39176 16-91) New York, Pergamon Press, Inc., 1978, p. 2049-2063.
- 314 Clanton, U.S., McKay, D.S., Waits, G., and Fuhrman, R. (1978) Sublimate morphology on
315 74001 and 74002 orange and black glassy droplets. In: *Lunar and Planetary Science*
316 *Conference*, 9th, Houston, Tex., March 13-17, 1978, Proceedings. Volume 2. (A79-
317 39176 16-91) New York, Pergamon Press, Inc., 1978, p. 1945-1957.
- 318 Cole, I.S., Muster, T.H., Furman, S.A., Wright, N., and Bradbury, A. (2008) Products Formed
319 during the Interaction of Seawater Droplets with Zinc Surfaces: I. Results from 1- and
320 2.5-Day Exposures. *Journal of The Electrochemical Society*, 155(5), C244-C255.
- 321 Day, J.M.D., Moynier, F., and Shearer, C.K. (2017) Late-stage magmatic outgassing from a
322 volatile-depleted Moon. *Proceedings of the National Academy of*
323 *Sciences*. DOI:10.1073/pnas.1708236114
- 324 Delano, J.W. (1986) Pristine lunar glasses: Criteria, data and implications. *Journal of*
325 *Geophysical Research* 91, D201-D213.
- 326 Diler, E., Rouvellou, B., Rioual, S., Lescop, B., Nguyen Vien, G., and Thierry, D. (2014)
327 Characterization of corrosion products of Zn and Zn-Mg-Al coated steel in a marine
328 atmosphere. *Corrosion Science*, 87, 111-117.

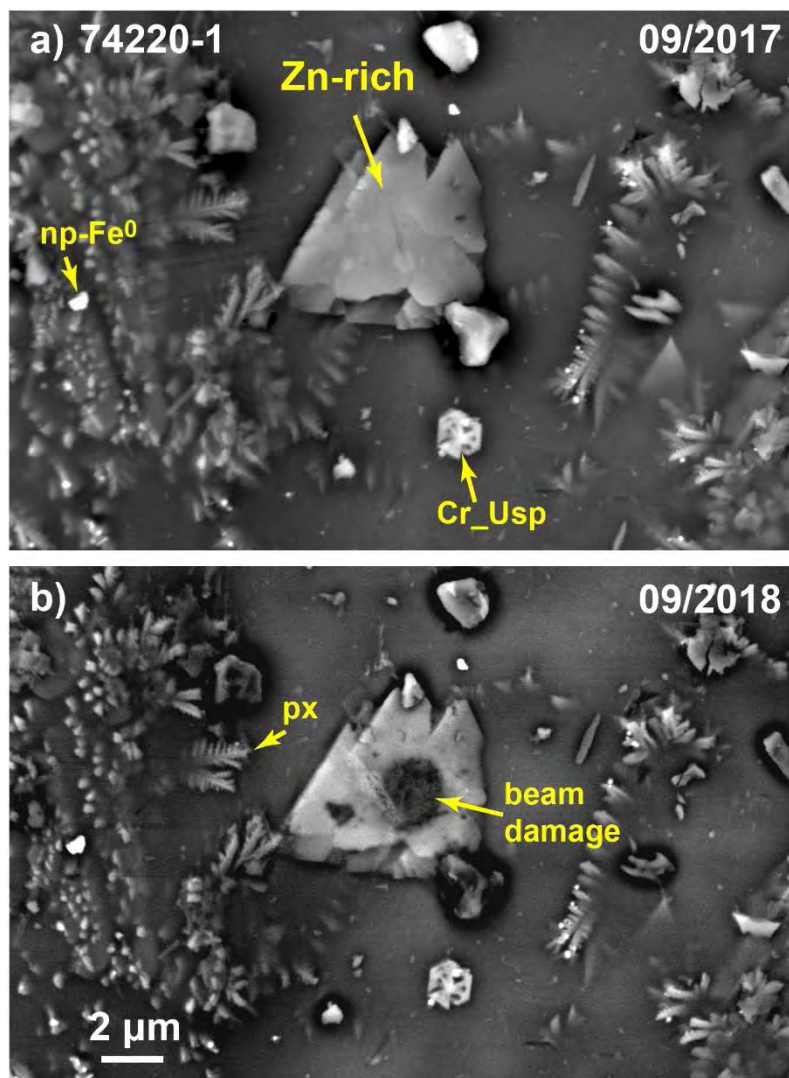
- 329 Ding, T.P., Thode, H.G., and Rees, C.E. (1983) Sulphur content and sulphur isotope composition
330 of orange and black glasses in Apollo 17 drive tube 74002/1. *Geochimica et*
331 *Cosmochimica Acta*, 47, 491-496.
- 332 Epstein, S., and Taylor, H.P., Jr. (1973) The isotope composition and concentration of water,
333 hydrogen and carbon in some Apollo 15 and 16 soils and in the Apollo 17 orange soil.
334 *Proceedings of the Fourth Lunar Science Conference, Supplement 4, Geochimica et*
335 *Cosmochimica Acta*, 2, 1559-1575.
- 336 Goldberg, R.H., Tombrello, T.A., and Burnett, D.S. (1976) Fluorine as a constituent in lunar
337 magmatic gases. In: *Lunar Science Conference, 7th, Houston, Tex., March 15-19, 1976,*
338 *Proceedings. Volume 2. (A77-34651 15-91) New York, Pergamon Press, Inc., p. 1597-*
339 *1613.*
- 340 Hauri, E.H., Weinreich, T., Saal, A.E., Rutherford, M.C., and Van Orman, J.A. (2011) High Pre-
341 Eruptive Water Contents Preserved in Lunar Melt Inclusions. *Science* 333, 213-215.
- 342 Heiken, G., and McKay, D.S. (1974) Petrography of Apollo 17 soils. In: *Lunar Science*
343 *Conference, 5th, Houston, Tex., March 18-22, 1974, Proceedings. Volume 1. (A75-*
344 *39540 19-91) New York, Pergamon Press, Inc., 1974, p. 843-860.*
- 345 Heiken, G.H., McKay, D.S., and Brown, R.W. (1974) Lunar deposits of possible pyroclastic
346 origin. *Geochimica et Cosmochimica Acta*, 38, 1703-1718.
- 347 Herzog, G.F., Moynier, F., Albarède, F., and Berezhnoy, A.A. (2009) Isotopic and elemental
348 abundances of copper and zinc in lunar samples, Zagami, Pele's hairs, and a terrestrial
349 basalt. *Geochimica et Cosmochimica Acta*, 73, 5884-5904.
- 350 Housley, R.M., Grant, R.W., and Cirlin, E.H. (1979) XPS and SAM studies of the surface
351 chemistry of lunar impact glasses including 12054. In: *Lunar and Planetary Science*
352 *Conference, 10th, Houston, Tex., March 19-23, 1979, Proceedings. Volume 2. (A80-*
353 *23617 08-91) New York, Pergamon Press, Inc., 1979, p. 1483-1490.*
- 354 Hui, H., Hess, K.-U., Zhang, Y., Nichols, A.R.L., Peslier, A.H., Lange, R.A., Dingwell, D.B.,
355 and Neal, C.R. (2018) Cooling rates of lunar orange glass beads. *Earth and Planetary*
356 *Science Letters*, 503, 88-94.
- 357 Kato, C., Moynier, F., Valdes, M.C., Dhaliwal, J.K., and Day, J.M.D. (2015) Extensive volatile
358 loss during formation and differentiation of the Moon. *Nature Communications* 6, 7617.
- 359 McKay, D.S., and Wentworth, S.J. (1992) Morphology and Composition of Condensates on
360 Apollo 17 Orange and Black Glass. In G. Ryder, H.H. Schmitt, and P.D. Spudis, Eds.
361 *Workshop on Geology of the Apollo 17 Landing Site, Part 1. LPI Technical Report 92-*
362 *09, Part 1, p. 31. Lunar and Planetary Institute, Houston, Texas.*
- 363 McKay, D.S., Clanton, U.S., and Ladle, G.H. (1973) Scanning electron microscope study of
364 Apollo 15 green glass. *Proceedings of the 4th Lunar Science Conference. Suppl. 4,*
365 *Geochimica et Cosmochimica Acta*, 1, 225-238.
- 366 Meyer, C., Jr., McKay, D.S., Anderson, D.H., and Butler, P., Jr. (1975) The source of sublimates
367 on the Apollo 15 green and Apollo 17 orange glass samples. In: *Lunar Science*
368 *Conference, 6th, Houston, Tex., March 17-21, 1975, Proceedings. Volume 2. (A78-*
369 *46668 21-91) New York, Pergamon Press, Inc., 1975, p. 1673-1699. 2, 1673-1699.*
- 370 Moynier, F., Albarède, F., and Herzog, G.F. (2006) Isotopic composition of zinc, copper, and
371 iron in lunar samples. *Geochimica et Cosmochimica Acta*, 70, 6103-6117.
- 372 Nasdala, L., Witzke, T., Ullrich, B., and Brett, R. (1998) Gordaite [Zn₄Na(OH)₆(SO₄)Cl·6H₂O]:
373 Second occurrence in the Juan de Fuca Ridge, and new data. *American Mineralogist*, 83,
374 p. 1111.

- 375 Odnevall, I., and Leygraf, C. (1993) Formation of $\text{NaZn}_4\text{Cl}(\text{OH})_6\text{SO}_4 \cdot 6\text{H}_2\text{O}$ in a marine
376 atmosphere. *Corrosion Science*, 34(8), 1213-1229.
- 377 Paniello, R.C., Day, J.M.D., and Moynier, F. (2012) Zinc isotopic evidence for the origin of the
378 Moon. *Nature*, 490, 376.
- 379 Renggli, C.J., King, P.L., Henley, R.W., and Norman, M.D. (2017) Volcanic gas composition,
380 metal dispersion and deposition during explosive volcanic eruptions on the Moon.
381 *Geochimica et Cosmochimica Acta*, 206, 296-311.
- 382 Saal, A.E., Hauri, E.H., Lo Cascio, M., Van Orman, J.A., Rutherford, M.C., and Cooper, R.F.
383 (2008) Volatile content of lunar volcanic glasses and the presence of water in the Moon's
384 interior. *Nature*, 454, 192-196.
- 385 Saal, A.E., Hauri, E.H., Van Orman, J.A., and Rutherford, M.J. (2013) Hydrogen Isotopes in
386 Lunar Volcanic Glasses and Melt Inclusions Reveal a Carbonaceous Chondrite Heritage.
387 *Science*, 340, 1317-1320.
- 388 Schlüter, J., Klaska, K.H., Friese, K., Adiwidjaja, G., and Gebhard, G. (1997) Gordaite,
389 $\text{NaZn}_4(\text{SO}_4)(\text{OH})_6\text{Cl} \cdot 6\text{H}_2\text{O}$, a new mineral from the San Francisco Mine, Antofagasta,
390 Chile. *Neues Jahrbuch Fur Mineralogie-Monatshefte*(4), 155-162.
- 391 Sharp, Z.D., Shearer, C.K., McKeegan, K.D., Barnes, J.D., and Wang, Y.Q. (2010) The chlorine
392 isotope composition of the Moon and implications for an anhydrous mantle. *Science*,
393 329, 1050-1053.
- 394 Tera, F., and Wasserburg, G.J. (1976) Lunar ball games and other sports. *Lunar and Planetary
395 Science Conference*, 7, p. 858.
- 396 Wasson, J.T., Boynton, W.V., Kallemeyn, G.W., Sundberg, L.L., and Wai, C.M. (1976) Volatile
397 compounds released during lunar lava fountaining. In: *Lunar Science Conference*, 7th,
398 Houston, Tex., March 15-19, 1976, Proceedings. Volume 2. (A77-34651 15-91) New
399 York, Pergamon Press, Inc., 1976, p. 1583-1595.
- 400 Wetzel, D.T., Hauri, E.H., Saal, A.E., and Rutherford, M.J. (2015) Carbon content and degassing
401 history of the lunar volcanic glasses. *Nature Geoscience*, 8, 755-758.
- 402 Wu, Z., Sun, X., Xu, H., Konishi, H., Wang, Y., Wang, C., Dai, Y., Deng, X., and Yu, M. (2016)
403 Occurrences and distribution of “invisible” precious metals in sulfide deposits from the
404 Edmond hydrothermal field, Central Indian Ridge. *Ore Geology Reviews*, 79, 105-132.
- 405 Zhu, L., Seff, K., Witzke, T., and Nasdala, L. (1997) Crystal structure of
406 $\text{Zn}_4\text{Na}(\text{OH})_6\text{SO}_4\text{Cl} \cdot 6\text{H}_2\text{O}$. *Journal of Chemical Crystallography*, 27(5), 325-329.

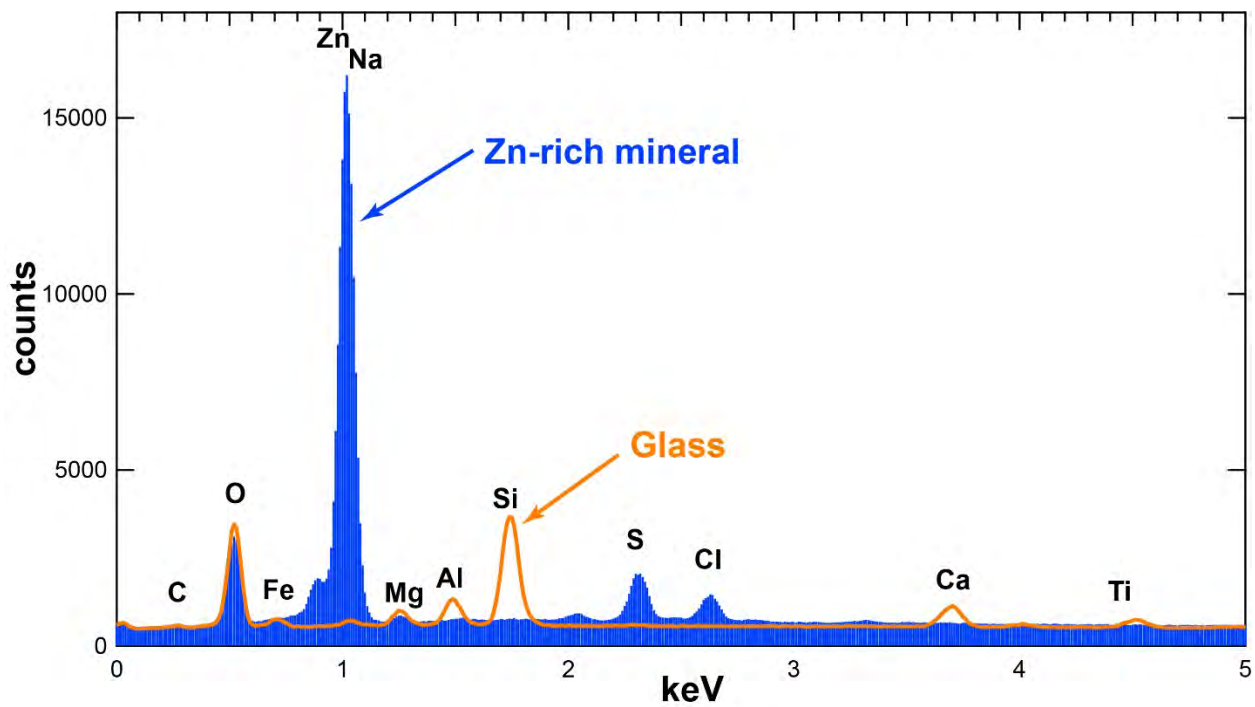


407
408
409
410
411
412
413
414
415
416

Figure 1. An example of the Zn-rich mineral on the surface of an orange bead from Stub 1 of 2017 sample mounts (imaged within ~9 days after original container was opened). (a) Backscattered electron image (BSE) of the bead showing the occurrences of the Zn-rich mineral (circles). (b) High magnification BSE image of the Zn-rich mineral (Zn-rich) showing platy crystals of a trigonal or hexagonal form. Nanometer pyroxene (px) and native iron (np-Fe⁰) are also present near the surface of the bead, which are likely quench crystals. The Zn-rich mineral lies above px and np-Fe⁰. This bead was imaged 15 months later and surface Zn-rich minerals show no changes (Fig. S3).



417
418 **Figure 2.** Comparison of Zn-rich grains imaged 12 months apart. a) A cluster of the Zn-rich
419 mineral each with a trigonal or hexagonal crystal shape on a volcanic bead (Fig. S1) that was
420 studied after exposing to the ambient air for ~3 months. b) The same cluster imaged after 15
421 months in the terrestrial air. Except for electron beam damages (dark regions on the cluster), other
422 regions of the cluster display no morphological and chemical changes. Other phases near the
423 surface are nanometer native Fe (np-Fe⁰), pyroxene (px), and chromian ulvöspinel (Cr_Usp),
424 which are likely quench crystals. Note that the isometric mineral (Cr-Usp) exhibits a different
425 form (skeletal) from the Zn-rich grains.



426

427 **Figure 3.** EDS spectra of the Zn-rich mineral and the glass substrate (see Fig. S2 of EDS locations).

428 **Table 1.** Representative composition of the Zn-rich mineral.*

Element	wt%	atom%
<i>O</i> <i>calculated</i>	26	53
Zn	58.3 ± 0.3	29.1
Na	5.2 ± 0.2	7.5
Mg	0.4 ± 0.1	0.6
S	6.1 ± 0.1	6.2
Cl	4.0 ± 0.1	3.7

429 *Uncertainties are one sigma values based on counting statistics.